Effect of Surface Motion on the Rotational Quadrupole Alignment Parameter of D_{2} Reacting on Cu(111)

Francesco Nattino, Cristina Díaz, Bret Jackson, and Geert-Jan Kroes

Phys. Rev. Lett. **108**, 236104 — Published 8 June 2012

DOI: 10.1103/PhysRevLett.108.236104

Effect of surface motion on the rotational quadrupole alignment parameter of D_2 reacting on Cu(111).

Francesco Nattino[1], Cristina Díaz[2], Bret Jackson[3], and Geert-Jan Kroes[1]

1: Leiden Institute of Chemistry, Gorlaeus Laboratories, Leiden University, P.O. Box 9502, 2300 RA Leiden, The Netherlands

2: Departamento de Química Módulo 13, Universidad Autónoma de Madrid, 28049 Madrid, Spain

3: Department of Chemistry, University of Massachusetts, Amherst, Massachusetts 01003, USA

Abstract. Ab-initio molecular dynamics (AIMD) calculations using the specific reaction parameter approach to density functional theory are presented for the reaction of D_2 on Cu(111) at high surface temperature (T_s =925 K). The focus is on the dependence of reaction on the alignment of the molecule's angular momentum relative to the surface. For the two rovibrational states for which measured energy resolved rotational quadrupole alignment parameters are available, and for the energies for which statistically accurate rotational quadrupole alignment parameters could be computed, statistically significant results of our AIMD calculations are that, on average: (i) including the effect of the experimental surface temperature (925 K) in the AIMD simulations leads to decreased rotational quadrupole alignment parameters, and (ii) including this effect leads to increased agreement with experiment.

PACS: 68.43.Bc; 8265.+r; 34.35.+a.

Experiments on the alignment dependence of molecule-surface reactions yield detailed information on the interaction of molecules with surfaces [1-3]. Because the rotational alignment parameter of reacting molecules is connected with the local anisotropy of the potential energy surface (PES), measurements of this parameter in conjunction with theory can lead to the identification of the reaction site [4, 5]. Measurement of this parameter as a function of translational energy may also reveal important mechanistic information on, for instance, the importance of orientational steering for reaction [3].

The sensitivity of the alignment of reacting molecules to the details of the molecule-surface interaction makes experiments addressing this topic ideal for testing electronic structure theories that attempt to model this interaction. Such tests are highly relevant, and pose huge challenges. About 90% of the chemical manufacturing processes used worldwide employ heterogeneous catalysts [6]. However, the best *ab initio* theory that can now be used to map out PESs for elementary molecule-surface reactions, density functional theory (DFT) at the generalised gradient approximation (GGA) or meta-GGA level, can provide reaction barriers with an accuracy of no better than 2.2 kcal/mol for gas phase reactions [7]. Even this accuracy has only recently become available [7], and it is therefore not surprising that quantum dynamics calculations using DFT PESs on the rotational quadrupole alignment parameter of H_2 desorbing from metal surfaces such as Pd(100) [8] and Cu(111) [9, 10] have not yet been able to quantitatively reproduce the experiments.

Dihydrogen-metal surface systems are ideal for testing electronic structure methods as accurate reaction probabilities can be computed within the Born-Oppenheimer (BO) approximation [11]. Making the static surface approximation (neglecting energy transfer involving phonons) should likewise lead to accurate results for low surface temperature (T_s) [12]. Taking advantage of this, it was recently shown that specific reaction parameter

DFT (SRP-DFT) [13] allows a chemically accurate description (to within 1 kcal/mol ≈ 43 meV) of experiments on reaction of H_2 and D_2 in molecular beams, on the influence of the initial rovibrational state of H_2 on reaction, and on rotational excitation of H_2, in scattering from Cu(111) [9, 10]. However, a quantitative description of experiments on the rotational alignment parameter of D_2 desorbing from Cu(111) was not yet realized [10].

The failure was attributed to errors in the dynamical model (the Born-Oppenheimer static surface (BOSS) model), noting that the alignment experiments [3] were performed at high T_s. In the experiments D_2 was permeated through a copper crystal, and alignment parameters were measured for D_2 recombinatively desorbed from Cu(111) using linearly polarised laser light and time-of-flight techniques to achieve rovibrational state selectivity and translational energy (E) resolution. The use of the permeation technique dictated the use of a high T_s (925 K). Associative desorption experiments at this T_s have also been used to derive initial state-selected, degeneracy averaged dissociative chemisorption probabilities $R_{vj}(E)$ [14], which are closely related to alignment parameters (*vide infra*, v and j are the vibrational and rotational quantum numbers of D_2). Deriving parameters describing $R_{vj}(E)$ required the assumption that dissociative chemisorption and associative desorption are related by detailed balance. The experimentalists confirmed the validity of this assumption by showing that sticking probabilities measured in molecular beam experiments at low T_s (120 K) could be well fitted using the $R_{vj}(E)$ derived from associative desorption experiments, if the widhts of the $R_{vj}(E)$ curves were adjusted on the basis of existing knowledge regarding their dependence on T_s [14]. The detailed balance assumption is probably also valid for the fully initial state-selected resolved reaction probabilities R_{vjm_j} required for the computation of alignment parameters (*vide infra*, m_j is the magnetic rotational quantum number of D_2), and theorists have relied on this assumption in previous calculations [8, 10]. However, for D_2 + Cu(111) and H_2 -

metal systems in general, no information is available on how T_s affects R_{vjm_j}, and thereby the alignment parameter. Here our aim is to resolve this issue for D_2 + Cu(111).

Using approximate molecule-phonon models, the effect of phonons on reactive scattering has been studied with reduced dimensionality models for H_2 + Cu [12, 15, 16], and treating all six molecular degrees of freedom for H_2 + Pd surfaces [17, 18]. DFT calculations on H_2 + Cu(111) have shown that the molecule-phonon coupling intricately depends on the motion of both first and second layer Cu atoms [19]. This complicated dependence is best handled by a method allowing surface atom motion and computing forces on the fly, such as the Ab Initio Molecular Dynamics (AIMD) method, which was first used to compute probabilities for molecule-surface reactions by Groß and co. [20]. They investigated H_2 dissociation on surfaces with initial T_s = 0 K. By extending the application of AIMD to non-zero initial T_s, here we show that quantitatively accurate modeling of the alignment parameter of D_2 desorbing from metal surfaces requires incorporation of surface motion in the theory. We show this by demonstrating that including the effect of the high experimental T_s in the theory yields rotational alignment parameters for D_2 + Cu(111) that, on average, differ significantly from static surface model results for the two rovibrational D_2 states for which experimental results have been obtained. Including the effect of the high experimental T_s also significantly improves the overall agreement with experiment. The AIMD results also yield an improved description of the initial state selected reaction probability for D_2 + Cu(111).

The AIMD calculations were done using the ab-initio total-energy and molecular-dynamics program VASP [21-23]. The effect of T_s is modeled by an appropriate sampling of the initial coordinates and velocities of the Cu atoms in the surface layers [24]. Individual collisions are modeled through NVU simulations keeping the number of atoms N, the cell size V, and the total energy U constant, the approximation of omitting a

thermostat being appropriate for the direct scattering problem addressed here. In the simulations the dimensions of the unit cell parallel to the surface were increased by 1.54% relative to their theoretical 0 K values to describe the experimentally determined expansion of bulk Cu [25, 26]. More details are provided in [24].

Assuming detailed balance, the rotational quadrupole alignment parameter for associative desorption was computed using [5]

$$A_0^{(2)}(j) = \frac{A}{B} = \frac{\sum_{m_j} R_{vjm_j}(E)\{3m_j^2 - j(j+1)\}/\{j(j+1)\}}{\sum_{m_j} R_{vjm_j}(E)} \qquad (1)$$

with the denominator B being equal to $(2j+1)R_{vj}$, and the quantum numbers referring to the initial state of D_2. $A_0^{(2)}(j)$ is positive if the molecule prefers to react with its bond axis parallel to the surface (helicopter rotation, $|m_j| = j$), negative if the molecule prefers to react end-on (cartwheel rotation, $m_j = 0$), and 0 if reaction is independent of orientation. In all theoretical results shown here, errors and error bars represent 68.3% confidence intervals. Calculations were done for the two D_2 rovibrational states investigated experimentally, at E values for which statistically accurate AIMD results could be obtained. The AIMD results were based on 3120 (1840) trajectories for the lowest E investigated for v=1,j=6 (v=0,j=11), and on half these amounts for the other E's.

For the two states for which energy resolved experimental results are available, the $A_0^{(2)}(j)$ values computed with AIMD are lower than the AIMD results computed for a fixed surface at 0 K (AIMDf) for all but one case ((v=1,j=6) at E = 0.6 eV, see Fig.1). An analysis [24] based on statistical hypothesis testing and the sum of the individual differences between the AIMD and AIMDf results divided by the standard errors in these

differences shows that, for the two rovibrational states addressed and the collision energies for which reasonably accurate AIMD results could be obtained, the AIMD results fall below the AIMDf results on average (significance level $\alpha = 0.05$). Modeling surface motion with AIMD also leads to a clear and statistically significant improvement in the overall agreement with experiment when comparing to the AIMDf results [24] and the previous quantum dynamical and quasi-classical BOSS results [9, 10]. On average, the AIMDf alignment parameters are significantly lower, and therefore in better agreement with experiment [24] than the previous QCT BOSS results, which we attribute to improvements in the static surface model achieved here through the AIMDf calculations and further discussed in [24]. Finally, we note that the similarity between the quantum dynamical and QCT BOSS results in Fig.1 validates the use of quasi-classical mechanics in AIMD [24] to compute $A_0^{(2)}(j)$).

In Fig.2 the AIMD results for $R_{vj}(E)$ are in much better agreement with experimentally fitted [14, 27] results for the (v=0,j=11) state at T_s=925 K than the previous QCT BOSS model results with experimentally fitted [14, 27] results for T_s=120 K [9, 10], for the lower E for which the experimental fits can be expected to be most reliable. The improvement may well be due in large part to improvements introduced in AIMD other than allowing surface motion [24], as the difference between the AIMD and AIMDf results is smaller than between AIMD and QCT/BOSS. The AIMD value of the energy E_0 (0.574 ± 0.009 eV) at which the reaction probability becomes equal to half the maximum experimentally fitted value (A=0.27 [27]) agrees with the experimental value (0.546 eV) to within chemical accuracy. AIMD calculations for additional rovibrational states are needed to establish whether the AIMD method can describe the experimental $E_0(v,j)$ values for D_2 with chemical accuracy for the greater part of the (v,j) states for which experimental results are available; only marginal improvement was observed for (v=1,j=6) here (Fig.2, the difference between the AIMD and experimental E_0 values is 45

meV). The comparison of the AIMD and AIMDf results is consistent with the finding of low-dimensional calculations using surface oscillator approximations [12, 16] and experiments [14, 28] that raising T_s broadens the reaction probability around a common midpoint.

The fact that $A_0^{(2)}(j)$ may be written as a fraction (Eq.1) suggests the existence of two distinguishable mechanisms that may lead to decrease of this parameter. Figure 3 illustrates these two mechanisms, for the (v=1,j=6) state. At the lowest E the denominator of the fraction increases because $R_{vj}(E)$ increases with T_s (see also Fig.2), leading to a decrease in $A_0^{(2)}(j)$ (Fig.1) even though cartwheel (low $|m_j|$) reaction probabilities do not increase more than helicopter (high $|m_j|$) reaction probabilities, leaving the numerator in Eq.1 almost unchanged [24] (mechanism I). The importance of this mechanism at low E [24] is consistent with DFT findings that the molecule-surface interaction is decreased in an isotropic fashion for the two lowest high symmetry barrier geometries (bridge-to-hollow and the t2h site halfway between a top and hcp site) if the closest second layer (or hcp) Cu atom moves down (see figure 9 of Ref.[19]). Such configurations will be increasingly available at high T_s. At these configurations the energy available to reaction (the molecule's energy minus the height of the barrier) is increased, whereas the "anisotropy energy" (which may be defined as the interaction energy of a tilted molecule minus that of a parallel molecule at the reaction barrier geometry [3]) is unchanged. Under these conditions, the reaction probability may be expected to increase by the same amount for all m_j (as seen in Fig.3 for 0.4 eV), which is consistent with the mechanism discussed above. A reasoning based on increasing available energy and unchanged anisotropy energy has also been invoked to explain the dependence of $A_0^{(2)}(j)$ on incidence energy [3].

Figure 3 shows that at the intermediate E of 0.5 eV the decrease in $A_0^{(2)}(j)$ (Fig.1) is due to increased reaction of states with low $|m_j|$ and decreased reaction of states with high $|m_j|$, leading to a decrease in the numerator of Eq.1 whereas the denominator is almost unchanged (it is actually decreased [24]), in what we call mechanism II. The above two cases represent ideal cases: in some cases a change in $A_0^{(2)}(j)$ reflects both changes in the preference for helicopter vs. cartwheel reaction and changes in $R_{vj}(E)$. We have also seen cases where changes in the numerator and the demoninator work in opposite ways but one of the effect dominates [24]. Our interpretation of mechanism II is as follows. On a cold surface, the preference found for reaction with D_2 parallel to the surface arises from the barrier being lowest in this alignment, because it best allows the D-atoms to simultaneously form bonds to the surface. On a hot surface the preference for parallel reaction is diminished because the molecule is more likely to encounter environments in which the surface is locally distorted, such that the simultaneous formation of D-metal bonds may be favored for tilted configurations. One would then expect increased reaction of states with low $|m_j|$ and decreased reaction of states with high $|m_j|$, whereas $R_{vj}(E)$ might remain unchanged.

The increase in $R_{vj}(E)$ in mechanism I is not only correlated with motion of the second layer Cu atom closest to the impinging D_2 molecule, but also to motion of the closest first layer Cu atom, because the barrier height is decreased for the lowest reaction barrier geometry if this Cu atom moves up [19]. Indeed, in reactive events, and for the initial states and energies at which mechanism I operates or an increase in $R_{vj}(E)$ contributes to a decreased alignment parameter [24], we observe significantly larger values Z_{12} of the vertical distance between these Cu-atoms than for scattering (Table 1). At the T_s considered here large Z_{12} values do not only result from large amplitude phonon motion, but also from thermal expansion: experiments show that the d_{12} interlayer distance goes up by 2.7 % going from 0 to 925 K, and our DFT and AIMD calculations reproduce this

trend. The large increase of d_{12} reflects both thermal expansion of the bulk (1.54 % [25, 26]) and d_{12} being contracted with respect to the bulk at low T_s, but bulk-like at high T_s [29]. The lowering of the barrier heights we see (Table 2) with increased tensile strain (T_s) may be explained [30] from the d-band model [31]: smaller overlap between substrate atoms reduces the width of the d-band, causing an upshift of the band if it is more than half-filled, which usually leads to higher reactivity.

The error bars on the experimental results in Fig.1 are estimates of confidence intervals based on an assessment of systematic errors that affect the energy calibration and limited information on statistical errors: They were based on noise in the time-of-flight spectra and uncertainties in the fits used, but on only one set (two sets) of measurements for v=1,j=6 (v=0,j=11) [32]. Conversely, the AIMD error bars only represent statistical errors. In the AIMD, systematic errors can arise from the use of too few Cu layers or a too small surface unit cell to adequately model surface motion. Considering the uncertainties in the experimental and theoretical error analyses, we argue that the best statement we can make presently about the agreement with experiment is that going from the BOSS model to the AIMD model, which allows the surface to move, the overall agreement is improved significantly. We believe that further theoretical work aimed at eliminating the systematic errors that may still be present in the AIMD is best performed when experimental results accompanied by a more complete error analysis become available. If the differences between theory based on the detailed balance assumption and associative desorption experiments persist, further research should be performed to address the validity of this assumption. For instance, it is possible that the permeation technique leads to an overestimated contribution of reaction involving D-atoms coming directly from the subsurface, which may be investigated with additional calculations, or using alternative techniques to dose D-atoms to the surface [28].

Acknowledgements. We thank D.J. Auerbach, A.M. Wodtke, S.M. Verduyn Lunel, M. Muskulus, and G. Nattino for useful discussions and helpful suggestions. C. Díaz gratefully acknowledges support under MICINN project FIS2010-15127 and CAM program NANOBIOMAGNET S2009/MAT1726. B. Jackson gratefully acknowledges support from the Division of Chemical Sciences, Office of Basic Energy Sciences, Office of Energy Research, U. S. Department of Energy, under Grant # DE-FG02-87ER13744. This research was supported by a grant of computing time from the stichting Nationale Computerfaciliteiten (NCF), and by a TOP-grant from Chemical Sciences (CW) of NWO.

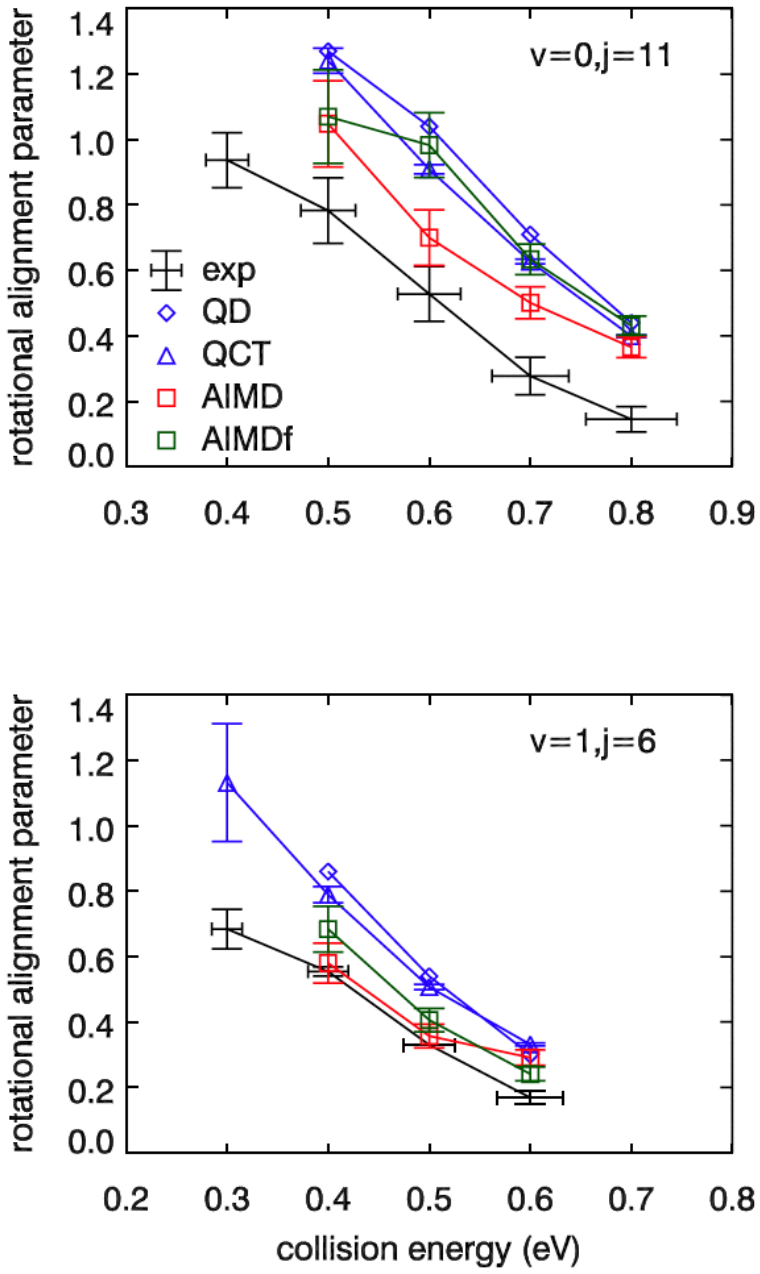

1. (Color) Comparison of $A_0^{(2)}(j)$ values measured in associative desorption experiments [3] with theoretical values computed using the AIMD method, the AIMD method with the surface held fixed at 0K (AIMDf), and with quantum dynamics (QD) and the QCT method using the BOSS model [9, 10].

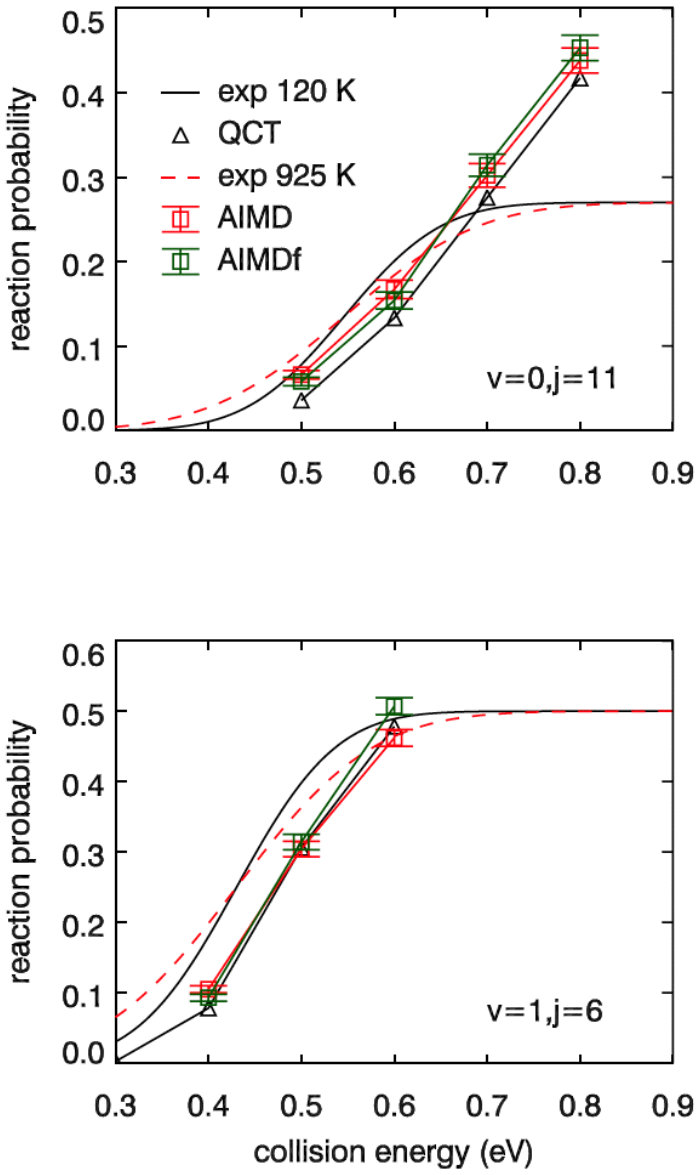

2. (Color) Comparison of experimentally fitted [14, 27] values of $R_{vj}(E)$ for T_s = 120 and 925 K with theoretical values computed using the AIMD and AIMDf methods and with the QCT method using the BOSS model [9, 10].

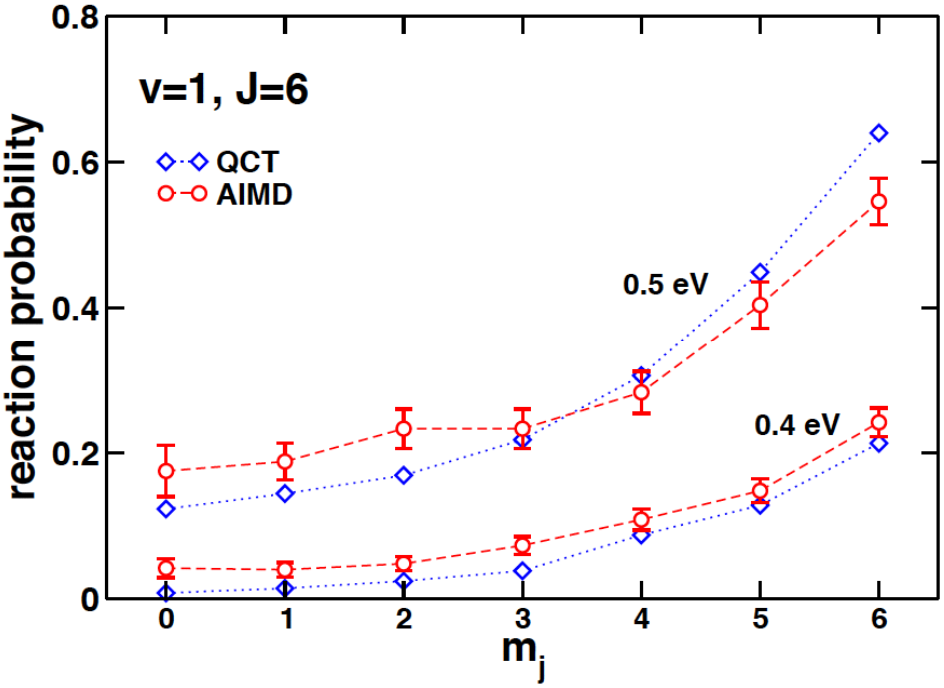

3. (Color) Comparison of $R_{vjm_j}(E)$ computed with AIMD with QCT results using the BOSS model [9, 10] for (v=1,j=6) D_2 + Cu(111).

Table 1. The average value of Z_{12} (in Å) and its error is shown for reacting D_2 (computed when r first becomes larger than 2.08 a_0, the value at the SRP minimum reaction barrier geometry [9]) and for scattering D_2 (computed at the largest outer turning point in r of scattering D_2).

D_2 state	E (eV)	Z_{12}^{av}, reaction	Z_{12}^{av}, scattering
v=1,j=6	0.4	2.273 ± 0.012	2.194 ± 0.004
v=0,j=11	0.5	2.292 ± 0.022	2.196 ± 0.005
v=0,j=11	0.6	2.260 ± 0.019	2.182 ± 0.008

Table 2. Parameters describing slab geometry and molecule-surface interaction energies (E_b, in eV) obtained with DFT and the SRP48 functional [24] are presented for the bridge-to-hollow (bth) and top-to-bridge (ttb) dissociation routes at SRP reaction barrier geometries [9], for T_s = 0 and 925 K.

Parameter	925 K	0 K
d_{12}(Å)	2.16	2.10
a_{3D}(Å)	3.74	3.68
E_b(bth)	0.593	0.628
E_b(ttb)	0.865	0.877

References.

1 B.L. Yoder, R. Bisson, and R.D. Beck, Science 329, 553 (2010).

2 M. Rutkowski, D. Wetzig, and H. Zacharias, Phys.Rev.Lett. 87, 246101 (2001).

3 H. Hou, S.J. Gulding, C.T. Rettner, A.M. Wodtke, and D.J. Auerbach, Science 277, 80 (1997).

4 M. Rutkowski and H. Zacharias, Phys.Chem.Chem.Phys. 3, 3645 (2001).

5 D.A. McCormack, G.J. Kroes, R.A. Olsen, J.A. Groeneveld, J.N.P.v. Stralen, E.J. Baerends, and R.C. Mowrey, Chem.Phys.Lett. 328, 317 (2000).

6 I. Chorkendorff and J.W. Niemantsverdriet, Concepts of Modern Catalysis and Kinetics (Wiley-VCH Verlag GMBH & Co., Weinheim, 2003).

7 R. Peverati and D.G. Truhlar, J.Phys.Chem.Lett. 3, 117 (2012).

8 A. Dianat and A. Groß, Phys.Chem.Chem.Phys. 4, 4126 (2002).

9 C. Díaz, E. Pijper, R.A. Olsen, H.F. Busnengo, D.J. Auerbach, and G.J. Kroes, Science 326, 832 (2009).

10 C. Díaz, R.A. Olsen, D.J. Auerbach, and G.J. Kroes, Phys.Chem.Chem.Phys. 12, 6499 (2010).

11 P. Nieto, E. Pijper, D. Barredo, G. Laurent, R.A. Olsen, E.J. Baerends, G.J. Kroes, and D. Farías, Science 312, 86 (2006).

12 M. Dohle and P. Saalfrank, Surf.Sci. 373, 95 (1997).

13 Y.Y. Chuang, M.L. Radhakrishnan, P.L. Fast, C.J. Cramer, and D.G. Truhlar, J.Phys.Chem.A 103, 4893 (1999).

14 H.A. Michelsen, C.T. Rettner, D.J. Auerbach, and R.N. Zare, J.Chem.Phys. 98, 8294 (1993).

15 Z.S. Wang, G.R. Darling, B. Jackson, and S. Holloway, J.Phys.Chem.B 106, 8422 (2002).

16 Z.S. Wang, G.R. Darling, and S. Holloway, J.Chem.Phys. 120, 2923 (2004).

17 H.F. Busnengo, W. Dong, and A. Salin, Phys.Rev.Lett. 93, 236103 (2004).

18 H.F. Busnengo, M.A. Di Césare, W. Dong, and A. Salin, Phys.Rev.B 72, 125411 (2005).

19 M. Bonfanti, C. Díaz, M.F. Somers, and G.J. Kroes, Phys.Chem.Chem.Phys. 13, 4552 (2011).

20 A. Groß and A. Dianat, Phys.Rev.Lett. 98, 206107 (2007).

21 G. Kresse and J. Hafner, Phys.Rev.B 47, 558 (1993).

22 G. Kresse and J. Furthmüller, Comput.Mater.Sci. 6, 15 (1996).

23 G. Kresse and J. Furthmüller, Phys.Rev.B 54, 11169 (1996).

24. See supplemental material at for a detailed description.

25 F.R. Kroeger and C.A. Swenson, J. Appl. Phys. 48, 853 (1977).

26 I.E. Leksina and S.I. Novikova, Sov. Phys.-Solid State 5, 798 (1963).

27 C.T. Rettner, H.A. Michelsen, and D.J. Auerbach, Faraday Discuss. 96, 17 (1993).

28 M.J. Murphy and A. Hodgson, J.Chem.Phys. 108, 4199 (1998).

29 K.H. Chae, H.C. Lu, and T. Gustafsson, Phys.Rev.B 54, 14082 (1996).

30 S. Sakong and A. Groß, Surf.Sci. 525, 107 (2003).

31 B. Hammer and J.K. Nørskov, Surf.Sci. 343, 211 (1995).

32 D.J. Auerbach and A.M. Wodtke, private communication.